Intracranial pressure dynamics in patients with acute brain damage

M. Ursino, C. A. Lodi, S. Rossi and N. Stocchetti

You might find this additional info useful...

This article cites 16 articles, 1 of which can be accessed free at:
/content/82/4/1270.full.html#ref-list-1

This article has been cited by 3 other HighWire hosted articles

Cerebral hemodynamics during arterial and CO_2 pressure changes: in vivo prediction by a mathematical model
M. Ursino, A. Ter Minassian, C. A. Lodi and L. Beydon
Am J Physiol Heart Circ Physiol, November 1, 2000; 279 (5): H2439-H2455.
[Abstract] [Full Text] [PDF]

Modeling cerebral autoregulation and CO_2 reactivity in patients with severe head injury
Carlo Alberto Lodi, Aram Ter Minassian, Laurent Beydon and Mauro Ursino
Am J Physiol Heart Circ Physiol, May 1, 1998; 274 (5): H1729-H1741.
[Abstract] [Full Text] [PDF]

A simple mathematical model of the interaction between intracranial pressure and cerebral hemodynamics
Mauro Ursino and Carlo Alberto Lodi
J Appl Physiol, April 1, 1997; 82 (4): 1256-1269.
[Abstract] [Full Text] [PDF]

Updated information and services including high resolution figures, can be found at:
/content/82/4/1270.full.html

Additional material and information about *Journal of Applied Physiology* can be found at:
http://www.the-aps.org/publications/jappl

This information is current as of January 7, 2015.

Intracranial pressure dynamics in patients with acute brain damage

M. URSINO,[1] C. A. LODI,[1] S. ROSSI,[2] AND N. STOCCHETTI[3]
[1]Department of Electronics, Computer Science, and Systems, University of Bologna,
I-40136, Bologna; [2]First Service of Anaesthesiology and Intensive Care,
Civic Hospital, Parma; and [3]Neurosurgical Intensive Care, Ospeotale Maggiore
Policlinico IRCCS, Milan, Italy

Ursino, M., C. A. Lodi, S. Rossi, and N. Stocchetti.
Intracranial pressure dynamics in patients with acute brain
damage. *J. Appl. Physiol.* 82(4): 1270–1282, 1997.—The time
pattern of intracranial pressure (ICP) during pressure-
volume index (PVI) tests was analyzed in 20 patients with
severe acute brain damage by means of a simple mathemati-
cal model. In most cases, a satisfactory fitting between model
response and patient data was achieved by adjusting only
four parameters: the cerebrospinal fluid (CSF) outflow resis-
tance, the intracranial elastance coefficient, and the gain and
time constant of cerebral autoregulation. The correlation
between the parameter estimates was also analyzed to eluci-
date the main mechanisms responsible for ICP changes in
each patient. Starting from information on the estimated
parameter values and their correlation, the patients were
classified into two main classes: those with weak autoregula-
tion (8 of 20 patients) and those with strong autoregulation
(12 of 20 patients). In the first group of patients, ICP mainly
reflects CSF circulation and passive cerebral blood volume
changes. In the second group, ICP exhibits paradoxical
responses attributable to active changes in cerebral blood
volume. Moreover, in two patients of the second group, the
time constant of autoregulation is significantly increased
(>40 s). The correlation between the parameter estimates
was significantly different in the two groups of patients,
suggesting the existence of different mechanisms responsible
for ICP changes. Moreover, analysis of the correlation between
the parameter estimates might give information on the directions
of parameter changes that have a greater impact on ICP.

intracranial dynamics; pressure-volume index tests; cerebral
autoregulation; mathematical modeling

PRESSURE-VOLUME INDEX (PVI) tests are frequently used
in neurosurgical intensive care units to derive informa-
tion on intracranial pressure (ICP) dynamics in pa-
tients with severe brain damage. For these tests a
small amount of fluid (1–4 ml) is injected into or
withdrawn from the cranial cavity and the consequent
ICP time pattern is monitored. The basic assumption is
that the immediate ICP response to a volume load
provides information on the pressure-volume character-
istic of the craniospinal compartment (hence, on the
intracranial storage capacity), whereas the subsequent
ICP trend also reflects the status of the cerebrospinal
fluid (CSF) circulatory pathways.

Several authors, however, recently questioned this
approach (4, 12, 13), suggesting that the ICP time
pattern during PVI tests may also contain information
on cerebral hemodynamics and on the status of cerebro-
vascular autoregulation mechanisms. The rationale of
this idea is that, after bolus injection or withdrawal,
cerebral blood volume (CBV) may vary significantly,
and these variations superimpose themselves on those
caused by the initial volume load and by the subse-
quent CSF circulation. Hence, analysis of PVI tests
may lead to a misleading interpretation of intracranial
dynamics, if autoregulation mechanisms and the status
of cerebral vessels are not properly taken into account.

In practice, analysis of the ICP response to bolus
injection or bolus withdrawal requires use of a mathemati-
cal model including the main parameters of craniospinal
system dynamics. The value of these parameters is then
individually estimated by looking for a best fit between
model predictions and the actual patient's ICP tracings. In
the classic model of Marmarou et al. (18, 19), the best fit
can be achieved by using simple analytic equations, which
justifies the great popularity of this test in clinical practice.
However, the model of Marmarou et al. includes only
intracranial compliance, CSF circulation, and vascular
factors in the extracranial veins (i.e., venous sinus pres-
sure), whereas the role of cerebral autoregulation and
active CBV changes is not incorporated.

The use of more complex models, also covering some
aspects of cerebrovascular regulation, may improve the
interpretation of PVI tests. These models, however, cannot
be solved by simple analytic formulas; hence, we must
resort to an algorithmic approach. The latter is based on an
iterative procedure for parameter estimation that mini-
mizes a suitable cost function of the difference between
model predictions and patient clinical data (5). This kind of
approach was recently adopted by us for the interpretation
of PVI tests in patients with acute brain damage (24). We
suggested that not only intracranial compliance and CSF
outflow resistance but also the gain and time constant of
cerebral autoregulation can be estimated with sufficient
accuracy starting from the ICP response to multiple PVI
tests performed in rapid succession.

The model used in our previous work (24), however, is
too complex and computationally onerous to be rou-
tinely used in a clinical setting. Hence, we recently
developed a reduced model that incorporates the main
relationships between ICP, CSF circulation, intracra-
nial compliance, and arterial-arteriolar CBV changes
in much simplified terms. With that model we were able
to reproduce several important properties of ICP dynam-
ics, such as the occurrence of plateau waves, the ICP
increase after acute arterial hypotension, and the depen-
dence of PVI on cerebral vessel response (25).

The aim of this study is to test whether the reduced
model can be used for the analysis of real ICP tracings
in patients with acute brain damage. In particular, we
want to *1*) check the capacity of the model to simulate

and predict short-term ICP changes during PVI tests by adjusting only a few parameters (intracranial compliance, CSF outflow resistance, cerebral autoregulation gain, and time constant), *2)* assess the accuracy of the parameter estimates obtained from real clinical data, and *3)* inspect the possibility of discriminating between patients with normal and weak autoregulation by looking at the estimated parameter values and at their mutual correlation.

Finally, the main advantages and limitations of this approach are discussed, and lines for future investigation are pointed out.

METHODS

Clinical Procedure

ICP monitoring was instituted in comatose trauma patients admitted to an intensive care unit. The measurement was done through a system consisting of a ventricular catheter, a commercially available monitoring line (Cordis intraventricular pressure-monitoring catheter with stopcock, model 910–127), and a disposable transducer (monitoring kit MK 5–04DTNVF, Abbott) connected to a Siemens monitor (Sirecust 1281 model 8791137). Arterial pressure was simultaneously measured through a catheter inserted into the radial artery with the same monitoring device adopted for the ICP measurement. Arterial CO_2 pressure and arterial O_2 content were carefully controlled in each patient; in particular, mild hyperventilation was used, keeping arterial P_{CO_2} between 30 and 35 Torr, while arterial saturation of hemoglobin was kept at >97%. ICP and arterial pressure data were sent to a Macintosh IIcx computer through an analog-to-digital con-verter (MacLab, World Precision Instruments), sampled at a rate of 20 Hz, and stored in the hard disk. The sampling rate is acceptable, since the frequency content of pressure signals does not exceed 10 Hz. The silicone catheter was positioned in the surgical room; it was inserted into the frontal horn of a lateral ventricle and tunneled for ~5 cm under the scalp. All the pressure lines were filled with sterile saline; the transducer was zeroed, with the external acoustic meatus as a reference point. The pressure-volume maneuver consisted of the injection or withdrawal of 1–4 ml of saline, according to the bolus technique described by Marmarou et al. (18). In all the maneuvers the injection rate was ~0.66 ml/s. The patients were artificially ventilated and under continuous sedation; in the case of respiratory problems, myorelaxant drugs were added. The PVI was tested every 12 h for the duration of the ICP monitoring; to minimize the fluctuations of the waveform related to artificial ventilation, the injection or the withdrawal was done at the same point of the respiratory cycle, possibly during the expiration phase. During the testing and for 30 min before testing, every drug or nursing procedure that could influence the ICP was avoided. The clinical status of all patients examined in this study, including the Glasgow coma scale and computerized tomography scan, is shown in Table 1.

Model Identification

ICP tracings during PVI tests were analyzed in 20 patients with acute brain damage by means of the mathematical model presented previously (25). The analysis consisted of two parts: *1)* identification of the main parameters through a best fit between the model and in vivo results and *2)* analysis of the correlation between parameters to characterize the main mechanisms responsible for the observed ICP changes.

Table 1. *Clinical status of patients*

Patient No.	Gender	Age, yr	GCS Admission	GCS Best 1st day	CT Scan	ICP, mmHg Mean	ICP, mmHg Max	MAP, mmHg Mean	CPP, mmHg Mean	CPP, mmHg Min	PVI Mean	PVI Min	Modified GOS
1	M	51	9	8	Contusions	18	27	92	75	58	29.14	23	
2	M	50	7	5	Contusions	24	50	109	84	50	22.43	16	GR/MD
3	M	50	5	6	Contusions	16	37	80	64	48	34.87	18	SD
4	F	22	6	7	Subdural	24	59	101	66	26	24.43	18	GR/MD
5	M	17	5	5	Contusions	35	64	99	63	10	33.72	11	GR/MD
6	M	17	3	5	Contusions	13	28	104	90	68	28.33	22	SD
7	M	34	3	8	Diffuse damage	23	33	119	96	64	30.5	26	GR/MD
8	M	23	6	5	Epidural hematoma	19	40	83	64	40	20.87	13	GR/MD
9	M	71	4	5	Diffuse damage	17	40	100	83	40	29.66	18	Died
10	M	19	4	5	Diffuse damage	20	50	94	74	32	24.6	16	GR/MD
11	M	48	6	6	Subdural	22	50	90	68	53	16.75	12	GR/MD
12	F	17	3	5	Contusions	20	51	84	64	32	22.18	14	SD
13	M	53	3	3	Subdural hematoma	29	50	92	74	50	14.78	8	GR/MD
14	M	50	7	5	Diffuse damage	16	30	95	79	60	32.77	20	Died
15	M	54	7	8	Subdural	20	40	97	77	60	11.8	10	GR/MD
16	M	14	7	5	Contusions	19	52	79	70	42	24.72	15	GR/MD
17	M	49	7	7	Diffuse damage	16	42	113	87	47	16.81	7	
18	F	33	3	4	Subdural hematoma	23	70	89	66	28	16.15	8	GR/MD
19	M	15	7	7	Contusions	28	52	92	64	25	21.75	6	GR/MD
20	M	49	8	7	Contusions	30	74	111	82	33	15.5	10	GR/MD

GCS admission, Glasgow coma scale evaluated at admission; GCS 1st day, best Glasgow coma scale score recorded during 1st day after trauma; CT scan diagnosis, diagnosis based on 1st computed tomographic scan performed at admission [diffuse damage indicates signs of increased intracranial content (basal cisterns compressed or absent) with or without subarachnoid hemorrhage]; ICP mean, mean intracranial pressure averaged over entire recording period; ICP max, maximum intracranial pressure, lasting >5 min, measured during entire recording period; MAP mean, mean arterial pressure averaged during entire recording period; CPP mean, mean cerebral perfusion pressure averaged during entire recording period; CPP min, lowest cerebral perfusion pressure, lasting >5 min, measured during entire recording period; PVI mean, mean pressure-volume index evaluated over all tests during recording period; PVI min, lowest pressure-volume index obtained over all tests performed during recording period; GOS, Glasgow outcome scale evaluated 6 mo after trauma through interview: GR/MD, good recovery or moderate disability; SD, severe disability; in 2 cases (*patients 1* and *17*) it was impossible to assess outcome.

Two preliminary elaborations were performed on each clinical tracing. First, because the model does not account for the pulsating changes in CBV induced by the sphygmic wave or by respiration, but it can only reproduce the low-frequency ICP pattern (25), the systemic arterial pressure (SAP) and ICP waveform have been numerically filtered. To eliminate the sphygmic wave, we used a low-pass finite impulse response (FIR) filter with 128 coefficients [designed with the Hamming window technique (16) and cutoff frequencies at 1 Hz], while the respiratory wave was eliminated by means of a 5-s moving-average filter. An example of the ICP and SAP tracings before and after filtration is shown in Fig. 1.

As clearly shown in Fig. 1, the ICP tracings exhibit some significant peaks, which are positive in correspondence with the bolus injection maneuvers and negative during bolus withdrawal. These peaks might be caused by force transmitted from the syringe into the cranial cavity or might represent the real instantaneous effect of the bolus on ICP; in the latter case, the bolus would cause a disproportionate instantaneous ICP change that, in a few seconds, is accommodated by volume redistribution along the neuraxis and/or by a decrease in cerebral venous blood volume. Because neither of these phenomena was included in the model, the portions of the ICP tracings containing peaks have been cut off (i.e., they have not been considered in the identification procedure).

Finally, the filtered ICP and SAP signals were stored in the computer at a sampling period of 1 Hz to be elaborated subsequently by means of the minimization algorithm. Sinus venous pressure was maintained constant (6 mmHg) throughout the simulations.

Parameter estimation. Model parameters were estimated through an automatic procedure. Starting from an initial guess, some model parameters suitably chosen a priori are iteratively modified by a numerical algorithm to minimize a cost function of the difference between the model and in vivo results. Because statistical information on the measurement errors was not available, we adopted the classic least-square cost function (5), i.e.

$$F(\Theta) = \sum_{i=1}^{N} [P_{ic}^{(s)}(t_i) - P_{ic}^{(m)}(t_i, P_a(t_i), \dot{P}_a(t_i), I_i, \Theta)]^2 \qquad (1)$$
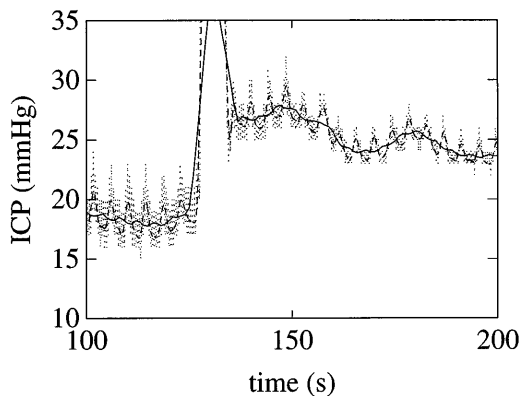

Fig. 1. An example of filtering cardiac and respiratory components on intracranial pressure (ICP) tracing of *patient 14*. Stippled line, original ICP response to a 2-ml bolus injection, with all pulsating components included. Dashed line, ICP tracing after elimination of sphygmic wave by low-pass filtering. Continuous line, ICP tracing when respiratory component was eliminated by means of a 5-s moving-average filter. Continuous line was used in identification procedure. Peak in clinical tracing is an artifact induced by maneuver that has not been considered in present work.

where $P_{ic}^{(s)}$ represents the filtered in vivo ICP value at the instant t_i, $P_{ic}^{(m)}$ is ICP model prediction at the same instant, P_a and $\dot{P}_a$ are the filtered SAP instant value and time derivative (to be used as inputs to the model), I_i is the bolus injection rate, N is the number of available data points, and $\Theta = [\theta_1, \theta_2, \ldots, \theta_p]^T$ is a vector of model parameters (including initial values of state variables) to be identified through the minimization algorithm.

The values of the parameters that warrant a local minimum for the cost function (i.e., $\hat{\Theta}$) are deemed to characterize the patient's intracranial dynamics.

A crucial problem in the use of the minimization algorithm consists in the choice of the parameters to be optimized. Theoretically, all model parameters and all initial values of state variables should be adjusted in each patient to improve the fitting. The parameters of the model are the initial value of ICP and of arterial compliance [$P_{ic}(0)$ and $C_a(0)$, respectively], the CSF formation and outflow resistances (R_f and R_o), the intracranial elastance coefficient (k_E), the central gain and amplitude of the sigmoidal autoregulation characteristic and the autoregulation time constant (G, ΔC_a, and τ, respectively), the basal value of compliance (C_{an}), the basal CBF (q_n), and the resistance of the large cerebral veins (R_{pv}).

However, when we are dealing with a parameter identification problem, the best compromise must be found among three different requirements: *1*) a good fit between the model and experimental results (this generally improves by increasing the number of estimated parameters), *2*) the accuracy of parameter estimates (this generally worsens with the number of parameters), and *3*) the physiological and clinical relevance of the estimates.

To clarify these problems, we performed some preliminary computer tests by varying all the model parameters. These tests suggested that venous resistance plays a negligible role during PVI tests. Moreover, the same trials revealed that only R_o/R_f can be identified with sufficient accuracy. For these reasons, R_{pv} and R_f were maintained at their basal level throughout the subsequent simulations. Furthermore, in most patients (with only 2 exceptions, see RESULTS) cerebral perfusion pressure (CPP) varied only by a few mmHg during PVI tests. Hence, just the central slope of the autoregulation characteristic, but not its saturation level, could be identified. For this reason, q_n and ΔC_a were maintained at their basal value throughout the simulations. Estimation of ΔC_a, however, was necessary to provide accurate reproduction of the ICP pattern in the two patients who exhibited large CPP changes.

The parameters estimated in all patients were thus k_E, R_o, G, and τ. All these parameters summarize a different aspect of intracranial dynamics with distinct clinical implications. Finally, the parameter C_{an}, which represents the basal value of arterial-arteriolar compliance (hence, the basal value of CBV) was estimated in only one case. In most patients a good fit of the ICP tracings could be achieved by maintaining this parameter at its basal level.

Once a final least-square estimate was obtained using the iterative scheme, an approximate evaluation of the covariance matrix $V(\Theta)$ of the parameter estimates was computed by assuming (2, 5)

$$V(\hat{\Theta}) = \sigma^2 \cdot [S^T \cdot S]^{-1}$$

where σ^2 denotes the variance of the measurement noise (assumed equal for all the data points) and S is the $N \times p$ sensitivity matrix (where N is the number of data points and p is the number of parameters to be estimated) evaluated at

$\Theta = \hat{\Theta}$, i.e.

$$S = \left[\frac{\partial P_{ic}^{(m)}(t_i, P_a(t_i), \dot{P}_a(t_i), I_i, \Theta)}{\partial \Theta} \right]_{\Theta = \hat{\Theta}}$$

The sensitivity matrix was computed using a forward difference approximation for the time derivatives (7). As usual, σ^2 was estimated through the following equation

$$\sigma^2 = \frac{F(\hat{\Theta})}{N-p} = \frac{1}{N-p} \cdot \sum_{i=1}^{N} [P_{ic}^{(s)}(t_i) - P_{ic}^{(m)}(t_i, P_a(t_i), \dot{P}_a(t_i), I_i, \hat{\Theta})]^2$$

Knowledge of the covariance matrix is of paramount importance in any identification problem, since it provides a method for evaluating the accuracy of parameter estimates. Basically, the ith diagonal element of the covariance matrix, $v_{ii}(\hat{\Theta})$, represents the variance of the ith parameter estimate, $\hat{\theta}_i$. Starting from knowledge of the variance, the accuracy in the estimation of $\hat{\theta}_i$ was assessed by computing a 95% confidence interval for each estimated parameter, according to the following equation

$$\hat{\theta}_i \pm \sqrt{v_{ii}(\hat{\Theta})} \cdot t_{0.975}(df)$$

where df represents the degrees of freedom used in Student's distribution, i.e., $df = N - p$.

All the numerical computations described above (parameter estimation, evaluation of the covariance matrix, evaluation of confidence intervals) were performed on 486 MS-DOS personal computers using the free software ADAPT II developed at the University of Southern California (7).

Analysis of the correlation between parameters. In many cases, inspecting the confidence intervals of the estimates represents only a partial analysis, which does not exploit all the information contained in the covariance matrix. As is well known, the nondiagonal elements of V [i.e., the elements $v_{ij}(\hat{\Theta})$, with $i \neq j$], which were not used in the previous equations, provide information on the mutual correlation between the parameters θ_i and θ_j. As we attempt to demonstrate, analysis of this correlation may be of great clinical value in neurosurgical intensive care units.

A straightforward way for visualizing the correlation between parameters and for understanding its practical implications consists in computing the so-called ϵ-indifference regions of the parameter space. Let us assume that we have estimated the "best" values of model parameters ($\hat{\Theta}$); this is the value that minimizes the cost function $F(\Theta)$. A crucial question is, How much can we change the parameters simultaneously from their optimal value so that the cost function does not increase more than a given quantity ϵ? In other words, we look for the region of the parameter space that satisfies the following disequation

$$|F(\Theta) - F(\hat{\Theta})| < \epsilon \qquad (2)$$

The set of values of Θ that satisfies *Eq. 2* are commonly referred to as the ϵ-indifference region.

From our particular point of view, computation of the ϵ-indifference region is meaningful, since it provides information on how the parameters of intracranial dynamics can be modified together without affecting the ICP time pattern significantly. Even more important, analysis of the ϵ-indifference region permits us to make hypotheses on which concurrent changes in parameters may have the greatest effects on

ICP, hence, may be particularly dangerous or particularly beneficial for the patient's status.

The ϵ-indifference region can be approximated, in a sufficiently small neighborhood of the optimal value $\hat{\Theta}$ (i.e., if ϵ is small enough), by the following disequation

$$|d\Theta^T \hat{H} d\Theta| < 2\epsilon \qquad (3)$$

where $d\Theta$ denotes the vector of parameter changes with respect to the optimal value (i.e., $d\Theta = \Theta - \hat{\Theta}$) and $\hat{H}$ is the Hessian matrix evaluated at $\hat{\Theta}$. According to Bard (2), the Hessian matrix can be approximated by the reciprocal of the covariance matrix, i.e.

$$\hat{H} = V(\hat{\Theta})^{-1}$$

Equation 3 represents a family of ellipsoids in the p-dimensional parameter space. The ellipsoids corresponding to different values of ϵ are concentric, with equal shape and orientation; hence, the same essential information can be gained without paying attention to the particular value of ϵ. The ellipsoids can be visualized only when $p \leq 3$.

If only two parameters (i.e., θ_i and θ_j) are allowed to change simultaneously while all the others are set at their optimal value, one can visualize a two-dimensional section of the ϵ-indifference region. In the case of *Eq. 3*, this reduces to a simple ellipse.

In general, the orientation and the shape of these ellipses may be of importance (Fig. 2). If the axes of the ellipse are parallel to the θ_i and θ_j axes or if they have approximately the same length (Fig. 2B), the two parameters are uncorrelated. On the contrary, if the longest axis of the ellipse lies in the first and third quadrants of the plane (Fig. 2C), the two parameters are positively correlated; this means that the effect of increasing one parameter can be counterbalanced by increasing the other. Finally, if the longest axis lies in the second and fourth quadrants (Fig. 2A), the two parameters are negatively correlated; in this case, the effect of increasing one parameter can be counterbalanced by decreasing the other. Moreover, the degree of correlation between parameters is significantly related to the eccentricity of the ellipse: the higher the eccentricity (i.e., the ratio of the longest to the shortest axis), the more closely correlated the two parameters are.

From a clinical point of view, it is of particular importance to examine the directions of the longest and shortest axes, especially when the ellipses have great eccentricity. If the two parameters are modified simultaneously (by a therapeutic maneuver or by a patient's physiopathological change) so that their values move in the direction of the longest axis, the cost function exhibits only minor alterations; this means that the ICP time pattern is only scarcely sensitive to this particular combination of parameter changes. In contrast, if the two parameters vary simultaneously in the direction of the shortest axis, even small modifications in their values are able to elicit a considerable alteration in the cost function, hence, in the ICP time pattern.

Knowledge of the direction of maximum and minimum sensitivity for each patient may be of clinical value to avoid improper maneuvers causing unpredictable ICP changes and to plan the optimal target therapy for the ICP control.

Finally, the different orientations and eccentricity of the ϵ-indifference regions may enable better classification of patients and may provide suggestions on the main mechanisms responsible for ICP alterations during PVI tests (see RESULTS).
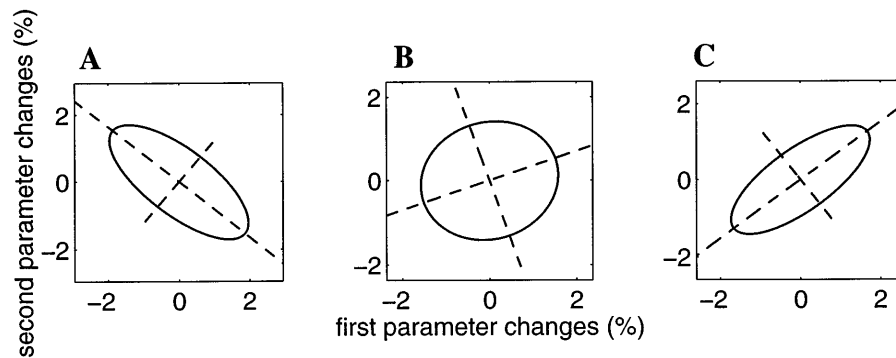
Fig. 2. Three qualitative examples of ϵ-indifference regions showing correlation between 2 hypothetical parameters of model. Inside region, cost function (hence, ICP percent changes) remains smaller than a given threshold, despite simultaneous alteration in 2 parameters. Longer axis of ellipse represents direction of minimum ICP sensitivity to parameter changes, whereas shorter axis gives direction of maximum sensitivity. *A*: 2 parameters are negatively correlated. ICP is only scarcely affected when 2 parameters change in opposite direction, but it is strongly affected when they change in same direction. *B*: 2 parameters are only scarcely correlated. *C*: 2 parameters are positively correlated. ICP is considerably affected when parameters change in opposite direction and scarcely affected when they change in same direction.

RESULTS

Parameter Identification

The basal value of all model parameters can be found in our previous work (Table 1 in Ref. 25). This value was assigned to all the parameters not individually estimated by the minimization algorithm. The values of parameters estimated in the 20 patients by means of the procedure described in METHODS are reported in Table 2. Each parameter is normalized with respect to the basal value to permit an immediate evaluation of the severity of its change. For each parameter, the 95% confidence interval is also reported.

Analysis of Table 2 suggests that, in most cases, the accuracy of parameter estimates is rather satisfactory. Only in a few instances can large values of confidence intervals be observed, indicating that the corresponding parameter is only poorly estimated with the ICP data available.

In Table 2, the k_E values vary from about one-half of normal (which means good intracranial compliance) to more than twice normal (poor compliance). These values are in the range reported in the clinical literature for patients with various intracranial diseases (1, 8, 9).

R_o is significantly increased in most patients. There is quite a strict correlation between basal ICP and R_o, suggesting that, in the model, CSF resistance is primarily responsible for sustained ICP. The R_o values reported in Table 2 agree reasonably well with those measured by Gjerris et al. (11) and Kosteljanetz (15) but are significantly higher than those reported by Marmarou and co-workers (17). Nevertheless, in a few

Table 2. *Parameter values*

Patient No.	R_o/R_{o0}	k_E/k_{E0}	G/G_0	τ/τ_0
1	4.300 Fixed	0.706 (0.661 ÷ 0.752)	0.103 (0.060 ÷ 0.146)	2.837 (2.118 ÷ 3.556)
2	8.098 (6.666 ÷ 9.530)	0.995 (0.840 ÷ 1.150)	0.516 (0.380 ÷ 0.652)	13.61 (7.466 ÷ 19.750)
3	3.675 (3.299 ÷ 4.052)	0.478 (0.456 ÷ 0.501)	0.764 (0.679 ÷ 0.848)	2.029 (1.638 ÷ 2.420)
4	9.804 (−3.897 ÷ 23.500)	1.447 (1.166 ÷ 1.728)	0.085 (0.063 ÷ 1.077)	0.214 (0.062 ÷ 0.366)
5	17.00 Fixed	1.303 (1.210 ÷ 1.396)	3.086 (2.660 ÷ 3.513)	0.131 (0.102 ÷ 0.160)
6	1.807 (1.721 ÷ 1.892)	0.445 (0.436 ÷ 0.454)	0.065 (0.045 ÷ 0.085)	0.139 (0.077 ÷ 0.200)
7	4.000 Fixed	0.548 (0.481 ÷ 0.614)	0.051 (0.034 ÷ 0.067)	13.01 (7.871 ÷ 18.150)
8	2.692 (2.552 ÷ 2.832)	1.337 (1.260 ÷ 1.413)	0.321 (0.310 ÷ 0.333)	0.187 (0.153 ÷ 0.221)
9	2.976 (2.248 ÷ 3.704)	0.719 (0.665 ÷ 0.773)	1.357 (−0.388 ÷ 3.102)	1.195 (0.846 ÷ 1.545)
10	5.173 (5.016 ÷ 5.330)	1.026 (1.000 ÷ 1.051)	0.952 (0.825 ÷ 1.078)	1.643 (1.353 ÷ 1.934)
11	9.006 (8.087 ÷ 9.925)	1.484 (1.400 ÷ 1.568)	0.130 (0.124 ÷ 0.137)	0.187 (0.152 ÷ 0.223)
12	3.324 (3.165 ÷ 3.484)	0.774 (0.751 ÷ 0.798)	0.612 (0.570 ÷ 0.654)	0.209 (0.104 ÷ 0.314)
13	1.061 (1.022 ÷ 1.099)	0.826 (0.807 ÷ 0.845)	0.074 (0.067 ÷ 0.080)	0.211 (0.152 ÷ 0.271)
14	4.339 (4.228 ÷ 4.450)	1.208 (1.177 ÷ 1.239)	0.425 (0.341 ÷ 0.510)	0.886 (0.687 ÷ 1.085)
15	3.508 (3.313 ÷ 3.720)	2.261 (2.188 ÷ 2.334)	0.142 (0.130 ÷ 0.153)	0.213 (0.169 ÷ 0.256)
16	3.474 (3.356 ÷ 3.593)	0.999 (0.970 ÷ 1.029)	0.237 (0.227 ÷ 0.247)	0.517 (0.389 ÷ 0.645)
17	5.505 (5.157 ÷ 5.854)	1.423 (1.388 ÷ 1.458)	0.299 (0.278 ÷ 0.321)	0.257 (0.188 ÷ 0.327)
18	8.392 (7.697 ÷ 9.087)	1.601 (1.492 ÷ 1.710)	0.345 (0.311 ÷ 0.378)	0.287 (0.235 ÷ 0.340)
19	10.710 (4.937 ÷ 16.480)	1.013 (0.721 ÷ 1.304)	0.108 (0.067 ÷ 0.150)	4.372 (1.111 ÷ 7.633)
20	19.950 (17.810 ÷ 22.080)	1.263 (1.066 ÷ 1.460)	0.522 (0.344 ÷ 0.700)	0.917 (0.465 ÷ 1.369)

R_o, cerebrospinal fluid outflow resistance; k_E, elastance coefficient; τ, time constant; C_a, arterial compliance; G, central gain. In *patient 5,* we also had to estimate $\Delta C_{an}/\Delta C_{an0}$ to reach an adequate fitting: $\Delta C_{an}/\Delta C_{an0} = 0.514$ (0.496 ÷ 0.531). In *patient 9,* we also had to estimate C_{an}/C_{an0} and $\Delta C_{an}/\Delta C_{an0}$ to reach an adequate fitting: $C_{an}/C_{an0} = 2.931$ (2.534 ÷ 3.328); $\Delta C_{an}/\Delta C_{an0} = 0.525$ (0.126 ÷ 0.923).
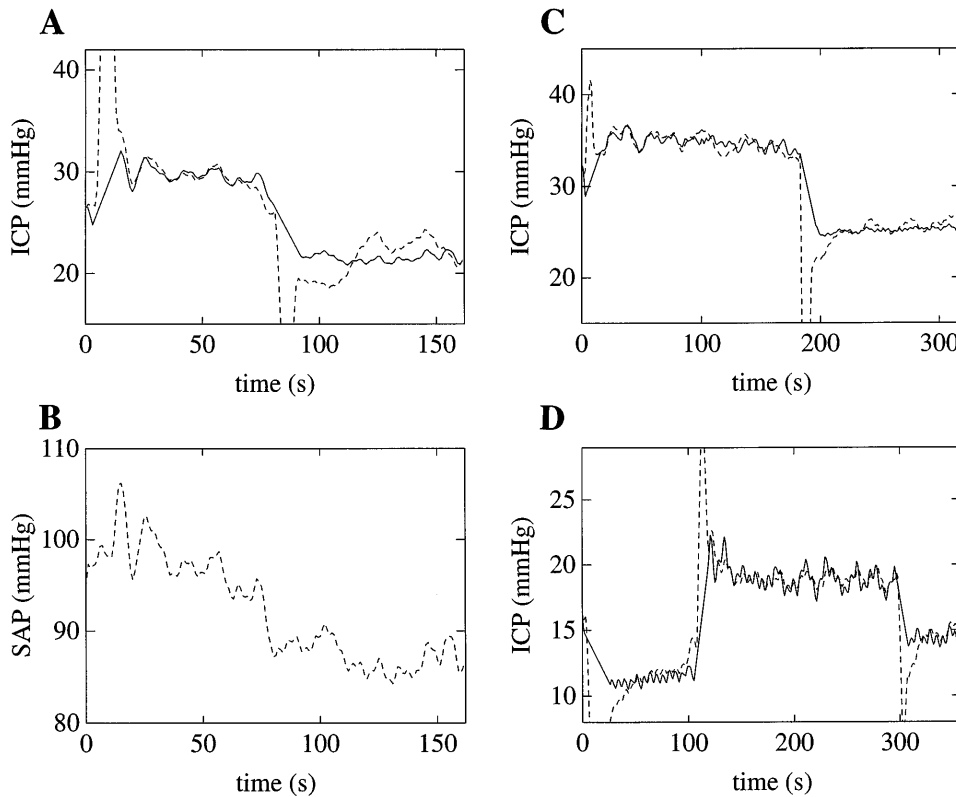
A

B

C

D

Fig. 3. Comparison of model ICP response (continuous line) with clinical data (dashed line) during pressure-volume index tests in 3 patients with weak autoregulation. In *patient 4*, mean systemic arterial pressure (SAP) used as input to model is also presented (*B*). All clinical curves were obtained by filtration of sphygmic and respiratory ICP waves. Positive and negative peaks in clinical tracings are artifacts induced by maneuvers. Amounts of mock cerebrospinal fluid injected and withdrawn in each trial were as follows: $+2$ and -2 ml for *patient 4* (*A* and *B*), $+2$ and -2 ml for *patient 11* (*C*), and -1, $+2$, and -1 ml for *patient 15* (*D*).

patients (*1, 5*, and *7*) R_o could not be estimated (i.e., the algorithm did not converge or the confidence interval of this parameter was extremely high), because these patients did not exhibit a constant ICP baseline before the maneuver. The absence of a well-defined baseline does not permit identification of the model equilibrium level, which is mainly related to the status of CSF circulation. In these situations, the minimization algorithm was run by setting R_o to a constant value that warrants an equilibrium level within the range of ICP fluctuations.

G and τ show large differences among patients: whereas a few patients exhibit quite normal values of these parameters, others are characterized by a moderate or severe reduction in G and/or by an increase in τ. The large individual variability in the estimated autoregulation response suggested that we roughly classify patients into three different classes: those with effective and prompt autoregulation ($G/G_0 > 0.2$, $\tau/\tau_0 < 2$), those with effective but slow autoregulation ($G/G_0 > 0.2$, $\tau/\tau_0 > 2$), and those with weak autoregulation ($G/G_0 < 0.2$). This classification, of course, is just indicative. As discussed in ϵ-*Indifference Regions*, better classification can be achieved by including the arterial-arteriolar blood volume among the estimated parameters and looking at the mutual correlation between the estimates.

Three examples of ICP tracings in patients classified with weak autoregulation are shown in Fig. 3. In these cases the ICP response to the maneuver shows a monotonic return toward the initial level (i.e., a monotonic decrease after bolus injection and a monotonic

increase after bolus withdrawal), as in the classic model of Marmarou et al. (18, 19). In *patient 4* the ICP response is also significantly modulated by the simultaneous decrease in SAP. The latter causes a passive reduction in CBV, which speeds the ICP decrease after bolus injection and opposes the ICP return to baseline after bolus withdrawal.

A few examples of ICP tracings in patients with preserved autoregulation are shown in Fig. 4, where *patients 8* and *14* are characterized by efficient and prompt autoregulation: after the bolus injection, ICP exhibits a sudden paradoxical response, which does, however, last for only a few seconds. After this period, active CBV changes are completed, and so the ICP progressively returns to the initial level owing to a prevalence of the CSF compensatory mechanisms. In contrast, *patient 3* is classified as having efficient but slow autoregulation: the paradoxical response develops progressively during the first minutes after the maneuver, according to the high τ. Finally, *patient 10* exhibits intermediate characteristics.

In 2 of 20 patients (i.e., *patients 5* and *9*) CPP (CPP = SAP $-$ ICP) displayed a significant reduction during PVI tests, approaching the autoregulation lower limit (50–60 mmHg). In these cases, reproduction of the ICP time patterns required identification not only of G but also of its saturation level. Moreover, in the case of *patient 9*, we also identified the total arteriolar blood volume. The results for these two patients are shown in Figs. 5 and 6 and are separately discussed below, since they are representative of the behavior of ICP at low CPP values close to the stability boundary.

Fig. 4. Comparison of model ICP response (continuous line) with clinical data (dashed line) during pressure-volume index tests in 4 patients with strong autoregulation. In particular, *patient 3* (*A*) has preserved autoregulation but slow dynamics; hence, paradoxical response lasts >1 min. *Patients 8* (*C*) and *14* (*D*) have preserved and rapid autoregulation; hence, paradoxical response lasts only a few seconds and is followed by a return to baseline due to cerebrospinal fluid circulation. *Patient 10* (*B*) shows intermediate characteristics. All clinical curves were obtained by filtration of sphygmic and respiratory ICP waves. Positive and negative peaks in clinical tracings are artifacts induced by maneuvers. Amounts of mock cerebrospinal fluid injected and withdrawn in each trial were as follows: +2, −2, and +2 ml for *patient 3*, +1 ml for *patient 8*, +2, −2, +1, and −2 ml for *patient 10*, and +2, −2, +2, and −2 ml for *patient 14*.
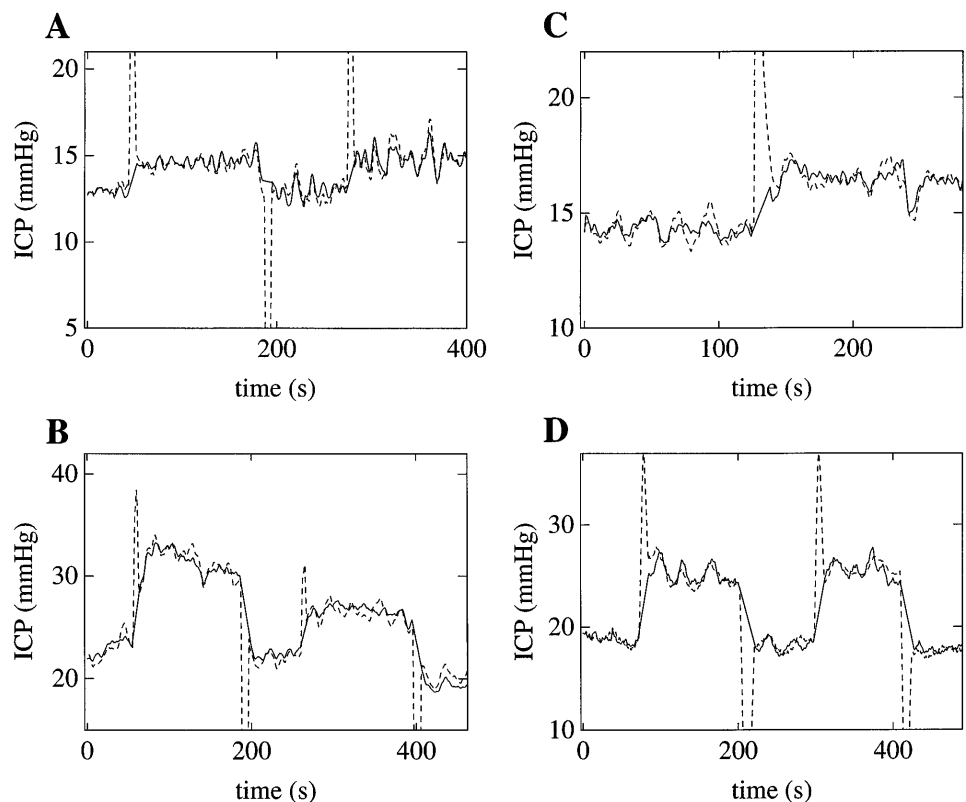
Figure 5 shows that the ICP of *patient 9* exhibits only a modest increase after the first bolus injection maneuver and a disproportionate increase after the second injection. The model ascribes the latter increase to the spontaneous SAP reduction during the final portion of the PVI test. As a consequence of the decrease in SAP, CPP approaches the lower autoregulation limit (84 − 25 ≃ 60 mmHg). In this pressure range, even a small fall in CPP is able to evoke a large increase in CBV (see Fig. 4 in Ref. 25), which, in turn, may be responsible for the disproportionate rise in ICP.

The ICP time pattern in *patient 5* (Fig. 6) is similar to that of a single aborted plateau wave. In this patient the bolus injection evokes an abrupt vasodilation and a consequent dramatic rise in ICP to ~50 mmHg. As a consequence, CPP falls below the autoregulation lower limit (CPP = 94 − 50 = 44 mmHg), a value that is maintained reasonably constant for >1 min. Finally, the bolus withdrawal causes a sudden vasoconstriction and the immediate restoration of ICP to a level quite close to the initial one. The slow increase in ICP evident in the last portion of the clinical tracing can be ascribed to a gradual vasodilation induced by the concomitant lowering of SAP.

ε-Indifference Regions

As discussed in METHODS, analysis of the mutual correlation between the parameter estimates and the construction of ε-indifference regions may be useful in reaching a more rigorous classification of patients and in formulating hypotheses on combinations of parameters that may have greater impact on ICP.

When investigating the mutual correlation between the parameters, however, we found that it was very beneficial to estimate not only R_o, k_E, the autoregulation central slope, and τ (which are the 4 parameters shown in Table 2), but also the total arterial-arteriolar blood volume (i.e., the basal value of arterial-arteriolar compliance). Inclusion of this additional parameter only scarcely improves the quality of fitting and worsens the accuracy of parameter estimates, but analysis of its correlation with the other parameters is worthwhile to discriminate between patients with strong and those with weak autoregulation.

For example, Fig. 7 shows some of the two-dimensional 5% indifference regions (obtained through *Eq. 3* with ε = 0.05) in *patients 4* and *11* (weak autoregulation). The same indifference regions are shown in Fig. 8 for *patients 3* and *9* (strong autoregulation). As clearly shown in Figs. 7 and 8, the orientation of most ellipses (hence, the correlation between parameters) is different in patients with weak and strong autoregulation. The reasons for these differences are briefly analyzed below. For simplicity, we focus attention only on the ICP time pattern after a bolus injection maneuver. Similar analyses can also be developed, of course, with reference to bolus withdrawal.

Correlation between the k_E and R_o. These two parameters exhibit a positive correlation in patients with weak autoregulation. In these patients, in fact, the return of ICP toward the baseline after bolus injection occurs according to a simple compliance plus resistance model; as is well known, the time constant of such a model is proportional to R_o/k_E. Hence, an identical time
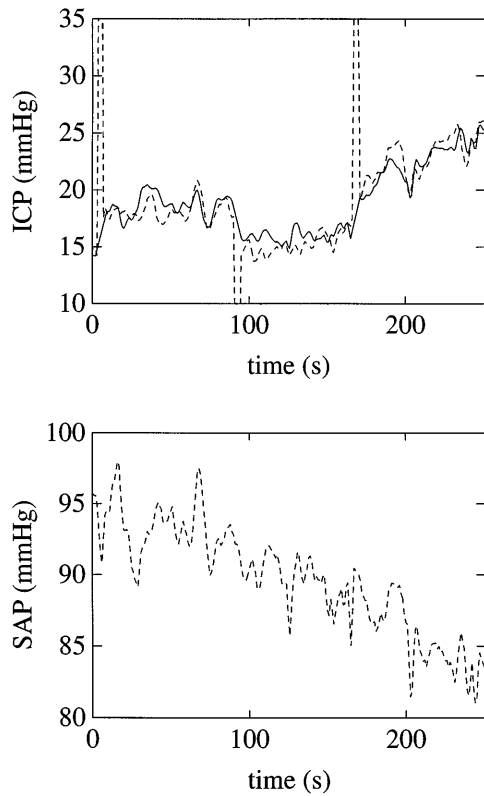
Fig. 5. *Top*: comparison of model ICP response (continuous line) with clinical data (dashed line) during pressure-volume index tests in a patient with strong but slow autoregulation (*patient 9*). *Bottom*: pattern of mean SAP, used as input to model. Disproportionate ICP increase is evident after last maneuver when SAP is decreasing and cerebral perfusion pressure approaches lower autoregulation limit. All clinical curves were obtained by filtration of sphygmic and respiratory ICP waves. Positive and negative peaks in clinical tracings are artifacts induced by maneuvers. Amounts of mock CSF injected and withdrawn were +2, −2, and +2 ml.

constant can be obtained by increasing R_o and k_E concurrently. In contrast, in patients with preserved autoregulation, an increase in k_E causes amplification of the paradoxical response to bolus injection, i.e., a further delayed ICP increase. The latter can be counteracted by improving CSF outflow, i.e., by decreasing R_o. The two parameters are thus inversely correlated in these patients.

Correlation between G and R_o. In Figs. 7 and 8, one can observe a negative correlation between these two parameters in the weak and strong autoregulation cases. In patients with weak autoregulation, an increase in G is reflected in an increase in CBF, which, in turn, causes an increased capillary pressure and an increased CSF production rate. The latter can be compensated for by decreasing R_o. In patients with preserved autoregulation, increasing G causes, besides the previous phenomenon, a stronger paradoxical increase in ICP after bolus injection. Both phenomena can be reduced by raising the CSF outflow, i.e., decreasing R_o.

Correlation between G and k_E. In patients with preserved autoregulation, these two parameters are inversely correlated. Increasing G causes a vasodila-

tion after bolus injection, with a consequent paradoxical increase in ICP. The latter can be compensated for by increasing the intracranial compliance, i.e., reducing k_E. In contrast, a clear correlation cannot be found in patients with weak autoregulation, where low eccentricity and contradictory orientation of the ellipses are observed.

Correlation of C_{an} with k_E, R_o, and G. As clearly shown in Fig. 7, in patients with weak autoregulation the correlation between C_{an} and the other three parameters is generally positive. Increasing C_{an} in the model means working with higher values of arterial-arteriolar blood volume. After a bolus injection, blood volume decreases passively in these patients, thus buffering the rise in ICP. The opposite effect (i.e., a further rise in ICP) occurs if R_o and/or G is increased. In these patients, however, the correlation between C_{an} and k_E is scanty. In contrast, in patients with strong autoregulation a higher arterial-arteriolar blood volume (hence, a higher C_{an}) causes a stronger paradoxical response after bolus injection. The latter can be attenuated by reducing R_o, i.e., permitting a more rapid CSF outflow,
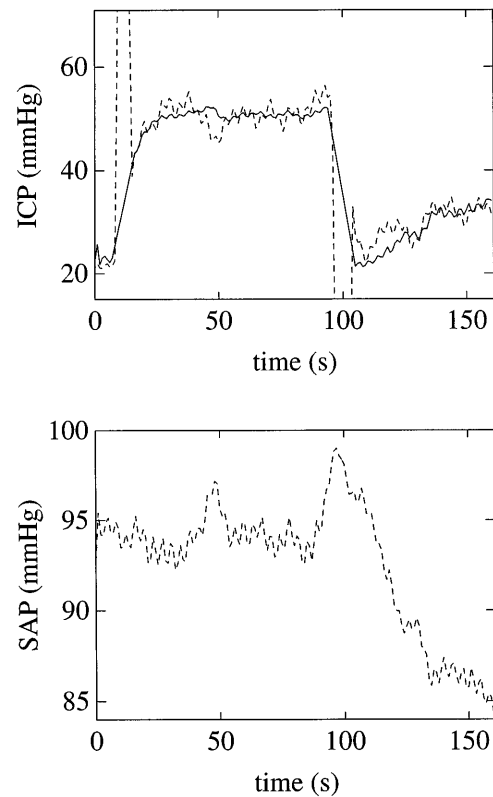

Fig. 6. *Top*: comparison of model ICP response (continuous line) with clinical data (dashed line) during pressure-volume index tests in a patient with strong and prompt autoregulation (*patient 5*). *Bottom*: pattern of mean SAP, used as input to model. ICP time pattern resembles a single plateau wave characterized by a sudden rise from an initial level to a level that exceeds lower autoregulation limit. Bolus withdrawal causes immediate abortion of wave. Final ICP increase is imputable to concomitant lowering of mean SAP. All clinical curves were obtained by filtration of sphygmic and respiratory ICP waves. Positive and negative peaks in clinical tracings are artifacts induced by maneuvers. Amounts of mock cerebrospinal fluid injected and withdrawn were +2 and −2 ml.
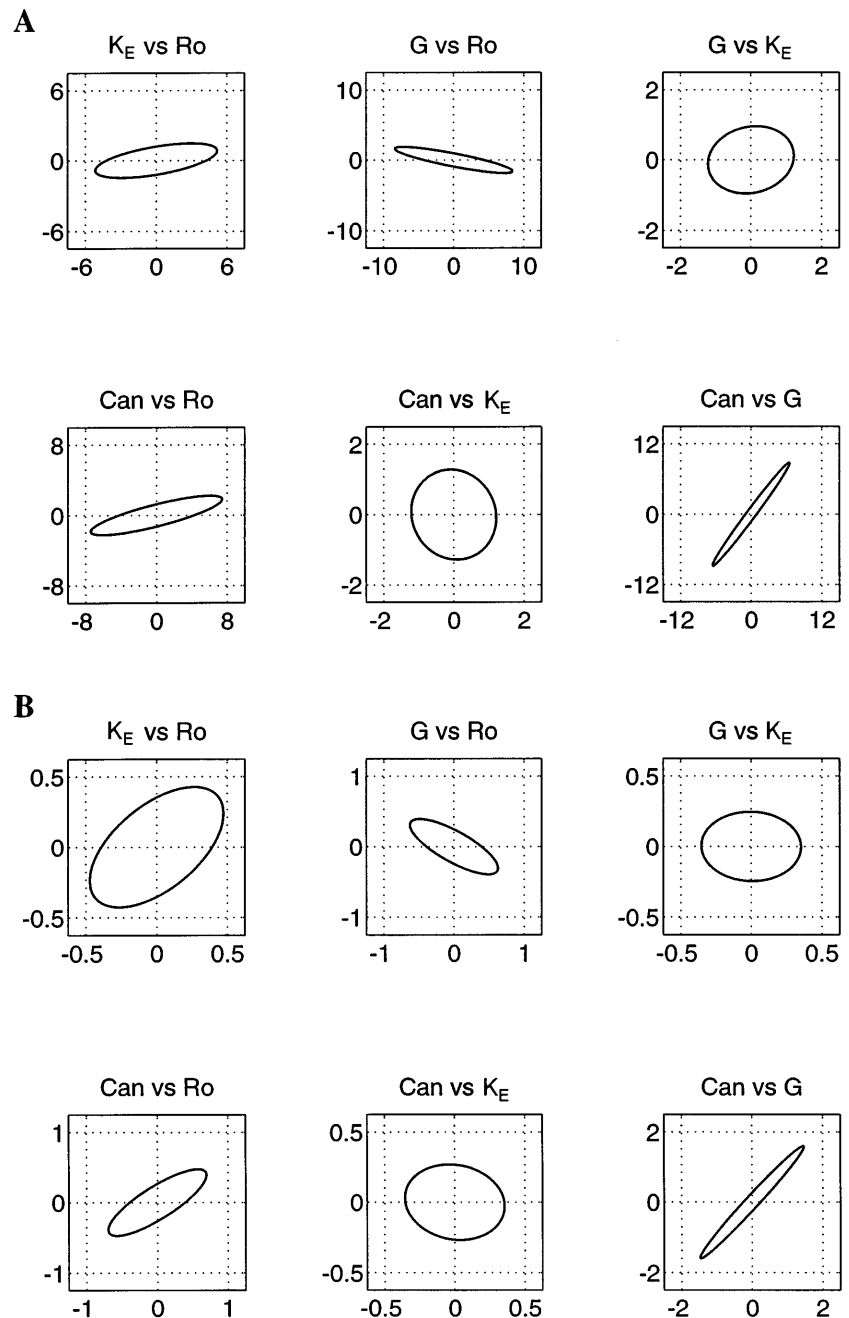
Fig. 7. 5% Indifference regions showing correlation between 2 parameters and effect of their simultaneous change on ICP in 2 patients with weak autoregulation [*patients 4* (*A*) and *11* (*B*)]. *x*- and *y*-Axes, parameter percent changes with respect to optimal value computed with minimization algorithm. Inside region, cost function varies by <5%; i.e., ICP changes are quite negligible. There is a positive correlation between intracranial elastance coefficient (k_E) and cerebrospinal fluid outflow resistance (R_o) and between arterial-arteriolar basal compliance (C_{an}) and R_o and/or autoregulation gain (G), because in weak autoregulation case, an increase in k_E and in C_{an} and an increase in G and R_o have opposite effects on ICP.

by reducing k_E, i.e., increasing intracranial compliance, or by reducing G. Hence, in these patients, C_{an} is inversely correlated with the other three parameters, as demonstrated by the inclination of the ellipses in Fig. 8.

DISCUSSION

The main result of the present work is that the proposed simple mathematical model of intracranial dynamics can reproduce the time pattern of ICP during PVI tests reasonably well by adjustment of only a few parameters with a clear clinical and physiological significance. Moreover, the model suggests that ICP during PVI tests contains information useful in charac-

terizing not only CSF dynamics and intracranial elastance but also the status of cerebrovascular autoregulation. Analysis of clinical tracings may permit hypotheses to be formulated on the most influential short-term mechanisms affecting ICP in a given patient and to point out their mutual relationships.

Traditionally, PVI tests are explained in terms of an intracranial compliance, loaded by a volume bolus, that progressively empties through the CSF circulatory pathways. This model gives rise to a simple monoexponential analytic relationship linking ICP during PVI tests to k_E and to R_o (18, 19). The clinical data available, however, suggest that the previous concepts are often oversimplified and can fail to grasp some important
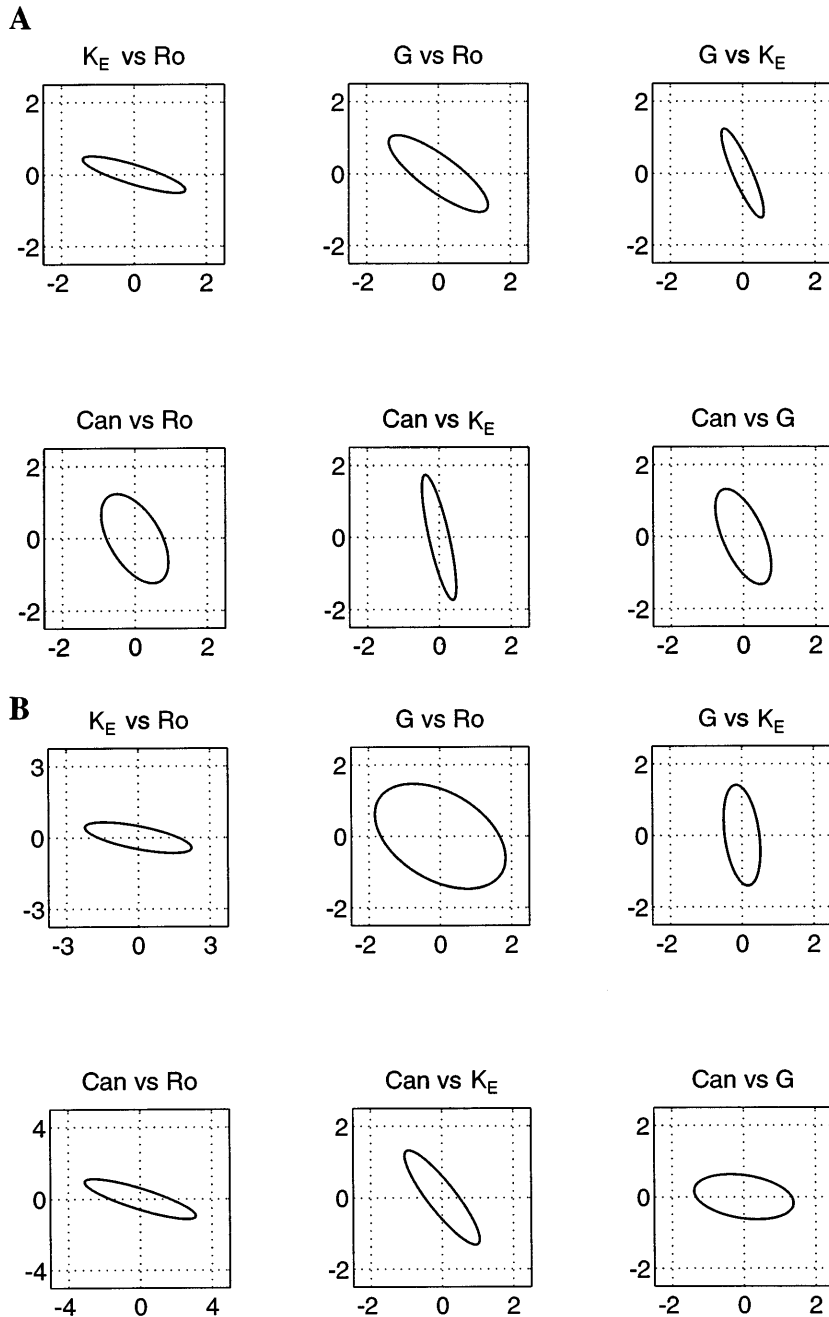
A

B

Fig. 8. 5% Indifference regions showing correlation between 2 parameters and effect of their simultaneous change on ICP in 2 patients with strong autoregulation [*patients 3* (*A*) and *9* (*B*)]. *x*- and *y*-Axes, parameter percent changes with respect to optimal value computed with minimization algorithm. Inside region, cost function varies by <5%; i.e., ICP changes are quite negligible. There is a negative correlation between all examined parameters, because in preserved autoregulation case, increasing any of these parameters causes ICP to change in same direction.

aspects of the ICP response, especially in patients with strong autoregulation mechanisms. Only in a limited number of cases does ICP exhibit a monotonic trend after the bolus injection or withdrawal maneuver, similar to that hypothesized in the traditional models. Consequently, we claim that more complex models are needed for the interpretation of PVI tests, also including some aspects of cerebral hemodynamics and CBV autoregulation adjustments.

During PVI tests, active CBV variations often manifest themselves through a paradoxical response, i.e., a delayed ICP increase after bolus injection and a delayed ICP reduction after withdrawal, through a mechanism analogous to the vasodilatory cascade described by Rosner and Becker (22). Although, in general, a

monotonic trend is characteristic of weak autoregulation whereas paradoxical responses are typical of patients with strong autoregulation, one must be aware that the ICP time pattern can also be significantly modulated by arterial pressure alterations during the trial (Figs. 3, 5, and 6). A correct classification of patients cannot be achieved simply by looking at the morphology of the ICP response, but by providing an overall fit of the model to clinical data and looking at the numerical values and mutual correlation of parameter estimates.

In 18 of 20 patients some portions of the ICP tracings were analyzed in a previous work by using a more complex model of the ICP dynamics (24). The results obtained here substantially confirm those reported

previously concerning the good fit and the kind of patient classification achieved. The significant improvement of the present study relative to the earlier study consists in far less computational effort being required to achieve parameter estimates owing to the drastic reduction in model complexity. We demonstrated that a reliable interpretation of PVI tests can be obtained by incorporating only a few fundamental mechanisms: a nonlinear storage capacity, CSF outflow, and an arterial-arteriolar compliance actively regulated by CBF changes. The possibility of using a reduced model without evident deterioration in its performance is of primary importance if one intends to apply the parameter estimation procedure directly in a clinical setting. Indeed, the complete model utilized previously (24) was too complex and computationally heavy to be of direct clinical advantage.

The parameter values estimated in this work agree quite closely with those reported in the clinical and physiological literature. The k_E is 0.05–0.25 ml^{-1} (Table 1). According to various authors (1, 8, 9), normal values for k_E are 0.05–0.15 ml^{-1}, whereas values as high as 0.25 ml^{-1} are often found in patients with severe brain disorders.

R_o is elevated in most patients (except *patient 13*, who exhibits a normal CSF outflow). In general, one can find quite a close relationship in our model between the basal ICP and R_o. This result agrees with the observations by Gjerris et al. (10, 11), Kosteljanetz (15), and Hansen et al. (14), who found a close correspondence between the measured ICP and R_o in patients with hydrocephalus and acute subarachnoid hemorrhage. In the present work most values of R_o are in the range 9.3–94.3 mmHg·ml^{-1}·min, except for *patients 5* and *20*, who have values as high as 132 and 175 mmHg·ml^{-1}·min, respectively. Similar values of R_o were reported by Hansen et al. (52–100 mmHg·ml^{-1}·min), Kosteljanetz (11.5–85 mmHg·ml^{-1}·min), and Borgesen et al. (3) (6.66–111.11 mmHg·ml^{-1}·min). In contrast, our results are not in agreement with the observation by Marmarou et al. (17), who found lower values of R_o (2.25–28.58 mmHg·ml^{-1}·min) in head-injured patients. Their values were able to account for only about one-third of the rise in ICP. The previous discrepancies might partly be imputable to differences between the steady-state infusion method (3, 14) and the bolus injection technique (17). Our model suggests that, during bolus injection tests, changes in CBV may significantly modify the ICP time course, thus affecting the estimation of R_o considerably. The latter effect, however, is probably much less important during steady-state infusion because of the different time constant of the maneuver with respect to that of CBV variations.

In all the trials examined, the bolus was injected at a high rate, i.e., the maneuvers lasted for just a few seconds. This is the protocol commonly adopted in neurosurgical units when PVI tests are performed. Moreover, when the identification procedure is performed, we used exactly the same injection rate in the model as in the patient. In the previous study, however, we demonstrated that the time course of active arterio-

lar blood volume changes and the nature of the delayed ICP increase may depend on the injection rate (25). It is thus possible that better estimation of model parameters may be gained in future work through a suitable choice of the rates for the maneuvers. This is the problem of the "optimal experiment design," which is crucial in all the parameter identification procedures (5). The choice of the optimum injection rates able to improve parameter estimation may be the subject of possible future refinements of this method.

According to the previous analysis, in the present work the main mechanism responsible for sustained ICP elevation is the increase in R_o. Furthermore, the mean ICP level in the model is also affected by CBF, hence, by the status of autoregulation mechanisms. CBF influences the CSF production rate through a change in intravascular pressure at the capillary level. Of course, there may be other mechanisms that elevate ICP and that have not been tested in this work, and they may become the subject of future refinements in the model and/or in the identification procedure. For instance, an increase in central venous pressure may affect ICP via a reduction in CSF outflow without the need for an increased resistance. This factor has not been included in this study, since, because of the lack of data, venous sinus pressure was maintained constant throughout the identification trials. Furthermore, changes in the osmotic pressure gradient may modulate CSF exchange at the capillary wall and may have sustained effects on ICP. Sustained ICP elevations in closed-head injury may also be the result of various mechanisms leading to increased intracranial content. These are often not well identified in clinical practice and are usually combined. Surgical masses, such as intracranial hematomas, are present in a relevant percentage of cases, and their expansion accounts for acute increases of ICP. In cases with focal lesions, such as cerebral contusions, the accumulation of fluid in the area surrounding the damaged tissue, mainly due to blood-brain barrier opening, may cause a significant rise in ICP. In diffuse damage it is more likely that a combination of vascular and nonvascular mechanisms causes an increase in intracranial content. Surgical masses have been identified and promptly evacuated in our cases; all our studies have been performed in a stable clinical situation, in which it may be assumed that a steady state has been reached.

In 12 of 20 patients the model ascribes part of the ICP response to active CBV changes induced by autoregulation mechanisms. In fact, these patients have quite a high autoregulation gain. In contrast, eight patients are classified as having weak autoregulation, since their autoregulation gain is lower than one-fifth of the basal value [the basal value of the autoregulation gain was assigned previously (25) as that value that warrants a constant CBF within the autoregulation range]. Finally, two patients classified with efficient autoregulation exhibit a significant increase in τ ($\tau \simeq 40$ s in *patient 3* and τ of a few minutes in *patient 2*). More generally, τ displays a large variability in the patients of the autoregulated group, ranging from a few seconds

to several 10ths of a second. The previous data confirm that autoregulation may be significantly altered in acute brain damage, a result reported by several authors (6, 21). Differences between prompt and delayed autoregulation might be ascribed to damage of neural control pathways (which generally have time constants of a few seconds), which are possibly replaced by the action of slower metabolic or chemical feedback mechanisms (20).

An important new element of the present work consists in the analysis of ϵ-indifference regions and of the corresponding correlation between parameter estimates. Although this technique is frequently used in engineering textbooks concurrently with identification problems (2), it has been applied only rarely in clinical practice until now. In our opinion, two main benefits encourage the use of this technique when the ICP patterns of patients with severe brain damage are analyzed.

1) By looking at the shape and orientation of the ellipses, one can formulate hypotheses on deep pathophysiological mechanisms responsible for ICP changes and, on this basis, attempt better patient classification. In Figs. 7 and 8 we demonstrated that patients can be differentiated by observing the orientation of the ellipses linking k_E with R_o, C_{an} with R_o, and C_{an} with G. A positive orientation is indicative of a prevalence of passive blood volume changes, hence, of weak autoregulation; a negative orientation suggests the prevalence of active blood volume alterations, hence, strong autoregulation mechanisms. The use of this criterion to differentiate patients in two classes leads to the same classification that can be achieved by looking at the autoregulation gain in Table 2, if $G/G_0 = 0.2$ is used for the classification threshold (i.e., if one assumes that patients with weak autoregulation have a gain smaller than $\frac{1}{5}$ of normal). Hence, the choice of this previous value for the classification threshold can be justified a posteriori as the value that warrants the best agreement between the classification and ellipse orientation.

2) Examination of the longer and shorter axes of the ellipses may permit the directions of maximum ICP sensitivity to parameter changes to be discerned. In perspective, this information might be exploited to design improved therapies for intracranial hypertension and to avoid inappropriate maneuvers in patients that risk acute ICP increase.

The previous possibilities arise from the definition of the ϵ-indifference region, i.e., the region of the parameter space where the cost function, $F(\Theta)$, exhibits only minor changes (below the threshold, ϵ) with respect to its optimum value. Because, according to *Eq. 1*, the cost function in our study depends only on the difference between model and clinical ICP, the ϵ-indifference region can be regarded as a region of relative insensitivity of ICP to parameter alterations. Moving along the longer axis, it is possible to modify parameters in a wide range without causing large alterations in ICP. In contrast, even a small parameter change in the direction of the shorter axis may have serious effects on ICP. The differences between the axis directions become more evident the more eccentric the ellipses are. Of course, the shorter axis gives only a clue of the direction of maximum ICP sensitivity. Whether ICP is actually increasing or decreasing depends on the movement along the axis.

The ellipses in Fig. 7 demonstrate that, in patients with weak autoregulation, the most important mechanism capable of buffering ICP changes is the passive blood volume alteration. Even a small decrease in C_{an}, which reduces the arterial blood volume initially contained in the craniospinal space, or a small increase in G, which makes the cerebrovascular bed behave less passively, may cause an important rise in the ICP response. This result agrees with findings of Gray and Rosner (12, 13), who observed a dramatic increase in PVI, hence, an improvement in the ICP response to bolus injection, when moving outside the autoregulation range. In contrast, in patients with strong autoregulation, active blood volume changes may induce paradoxical responses; as suggested by the direction of the shorter axes in Fig. 8, the paradoxical responses may be sharply amplified by an increase in the arterial-arteriolar basal compliance, G, k_E, and R_o. In the most serious cases (i.e., *patient 5* in Fig. 6) paradoxical responses may cause uncontrolled ICP increases similar to those occurring during the development of plateau waves. The previous considerations emphasize that patients with excessive cerebrovascular reactivity, reduced intracranial compliance, and poor CSF circulation may risk intracranial hypertension, and so any manipulation on these patients should be performed with extreme caution in intensive care units. Preliminary statistical tests performed on a wider patient population (34 patients) confirmed this result, indicating that patients with paradoxical responses to PVI tests generally have a worse outcome (23).

Finally, it is to be stressed that the previous analysis concerns only the acute ICP response to a bolus volume load; hence, it is indicative of only short-term intracranial dynamics. The model's usefulness lies in the possibility to reach a quantitative estimate of parameter values and to assess the tendency of the patient to develop uncontrolled acute intracranial hypertension in response to sudden perturbations. The possible role of other long-term mechanisms affecting ICP (e.g., osmosis, brain edema, tissue metabolism) has not been considered in the model, and so model simulation results cannot be used to achieve long-term forecasting of ICP derangement.

REFERENCES

1. **Avezaat, C. J. J., and J. H. M. van Eijndhoven.** The role of the pulsatile pressure variations in intracranial pressure monitoring. *Neurosurg. Rev.* 9: 113–120, 1986.
2. **Bard, Y.** *Nonlinear Parameter Estimation.* Orlando, FL: Academic, 1974.
3. **Borgesen, S. E., M. Albeck, F. Gjerris, M. Czonsnyka, and P. Laniewski.** Computerized infusion test compared to conven-

tional lumbo-ventricular perfusion for measurement of resistance to CSF outflow. In: *Intracranial Pressure VIII*, edited by C. J. J. Avezaat, J. H. M. van Eijndhoven, A. I. R. Maas, and J. T. J. Tans. Berlin: Springer-Verlag, 1993, p. 744–748.

4. **Bouma, G. J., J. P. Muizelaar, K. Bandoh, and A. Marmarou.** Blood pressure and intracranial pressure-volume dynamics in severe head injury: relationship with cerebral blood flow. *J. Neurosurg.* 77: 15–19, 1992.

5. **Cobelli, C., and J. DiStefano III.** Parameter and structural identifiability concepts and ambiguities: a critical review and analysis. *Am. J. Physiol.* 239 (*Regulatory Integrative Comp. Physiol.* 8): R7–R24, 1980.

6. **Cold, G. E., and F. T. Jensen.** Cerebral autoregulation in unconscious patients with brain injury. *Acta Anaesthesiol. Scand.* 22: 270–280, 1978.

7. **D'Argenio, D. Z., and A. Schumitzky.** *ADAPT II User's Guide.* Los Angeles, CA: Biomedical Simulation Resource, 1992.

8. **Delwel, E. J., D. A. de Jong, and C. J. J. Avezaat.** The relative prognostic value of CSF outflow resistance measurement in shunting for normal pressure hydrocephalus. In: *Intracranial Pressure VIII*, edited by C. J. J. Avezaat, J. H. M. van Eijndhoven, A. I. R. Maas, and J. T. J. Tans. Berlin: Springer-Verlag, 1993, p. 816–820.

9. **Eijndhoven, J. H. M. van, S. Sliwka, and C. J. J. Avezaat.** The constant pressure term (P0) of the volume-pressure relationship. Comparison between results of infusion test and pulse pressure analysis. In: *Intracranial Pressure VI*, edited by J. D. Miller, G. M. Teasdale, J. O. Rowan, S. L. Galbraith, and A. D. Mendelow. Berlin: Springer-Verlag, 1986, p. 48–53.

10. **Gjerris, F., S. E. Borgesen, E. Hoppe, F. Boesen, and A. M. Nordenbo.** The conductance to outflow of CSF in adults with high-pressure hydrocephalus. *Acta Neurochir.* 64: 59–67, 1982.

11. **Gjerris, F., S. E. Borgesen, P. S. Sorensen, F. Boesen, K. Schmidt, A. Harmsen, and J. Lester.** Resistance to cerebrospinal fluid outflow and intracranial pressure in patients with hydrocephalus after subarachnoid haemorrhage. *Acta Neurochir.* 88: 79–86, 1987.

12. **Gray, W. J., and M. J. Rosner.** Pressure-volume index as a function of cerebral perfusion pressure. 1. The effects of cerebral perfusion pressure changes and anesthesia. *J. Neurosurg.* 67: 369–376, 1987.

13. **Gray, W. J., and M. J. Rosner.** Pressure-volume index as a function of cerebral perfusion pressure. 2. The effects of low cerebral perfusion pressure and autoregulation. *J. Neurosurg.* 67: 377–380, 1987.

14. **Hansen, K., F. Gjerris, and P. S. Sorensen.** Absence of hydrocephalus in spite of impaired cerebrospinal fluid absorption and severe intracranial hypertension. *Acta Neurochir.* 86: 93–97, 1987.

15. **Kosteljanetz, M.** CSF dynamics in patients with subarachnoid and/or intraventricular hemorrhage. *J. Neurosurg.* 60: 940–946, 1984.

16. **Krauss, T. P., L. Shure, and J. N. Little.** *Signal Processing Toolbox for Use With MATLAB.* Natick, MA: MathWorks, 1994, p. 37–54.

17. **Marmarou, A., A. L. Maset, J. D. Ward, S. Choi, D. Brooks, H. A. Lutz, R. Moulton, J. P. Muizelaar, A. De Salles, and F. Young.** Contribution of CSF and vascular factors to elevation of ICP in severely head-injured patients. *J. Neurosurg.* 66: 883–890, 1987.

18. **Marmarou, A., K. Shulman, and J. LaMorgese.** Compartmental analysis of compliance and outflow resistance of the cerebrospinal fluid system. *J. Neurosurg.* 43: 523–534, 1975.

19. **Marmarou, A., K. Shulman, and R. M. Rosende.** A nonlinear analysis of the cerebrospinal fluid system and intracranial pressure dynamics. *J. Neurosurg.* 48: 332–344, 1978.

20. **Mchedlishvili, G.** *Arterial Behavior and Blood Circulation in the Brain.* New York: Plenum, 1986.

21. **Newell, D. W., R. Aaslid, R. Stooss, and H. J. Reulen.** Evaluation of closed head injury patients using transcranial Doppler monitoring. In: *Intracranial Pressure VIII*, edited by C. J. J. Avezaat, J. H. M. van Eijndhoven, A. I. R. Maas, and J. T. J. Tans. Berlin: Springer-Verlag, 1993, p. 309–312.

22. **Rosner, M. J., and D. P. Becker.** Origin and evolution of plateau waves. Experimental observation and a theoretical model. *J. Neurosurg.* 60: 312–324, 1984.

23. **Stocchetti, N., S. Rossi, P. Ceccarelli, M. Ursino, and D. Mancia.** Time pattern of ICP after bolus injection as an indicator of intracranial disturbances. In: *Intracranial Pressure IX*, edited by H. Nagai, K. Kamiya, and S. Ishii. Berlin: Springer-Verlag, 1993, p. 172–174.

24. **Ursino, M., M. Iezzi, and N. Stocchetti.** Intracranial pressure dynamics in patients with acute brain damage: a critical analysis with the aid of a mathematical model. *IEEE Trans. Biomed. Eng.* 42: 529–540, 1995.

25. **Ursino, M., and C. A. Lodi.** A simple mathematical model of the interaction between intracranial pressure and cerebral hemodynamics. *J. Appl. Physiol.* 82: 1256–1269, 1997.